Finite Elements in Analysis and Design 98 (2015) 26–40

Contents lists available at ScienceDirect

Finite Elements in Analysis and Design

journal homepage: www.elsevier.com/locate/finel

Finite strain quadrilateral shell using least-squares fit of relative Lagrangian in-plane strains☆

P. Areias [a,d,*], T. Rabczuk [b], J.M. César de Sá [c], J.E. Garção [a,e]

[a] Department of Physics, University of Évora, Colégio Luís António Verney, Rua Romão Ramalho, 59, 7002-554 Évora, Portugal
[b] Institute of Structural Mechanics, Bauhaus-University Weimar, Marienstraße 15, 99423 Weimar, Germany
[c] Mechanical Engineering Department, Faculty of Engineering, University of Porto, Rua Dr. Roberto Frias, s/n, 4200-465 Porto, Portugal
[d] ICIST, Lisbon, Portugal
[e] IDMEC, Lisbon, Portugal

ARTICLE INFO

Article history:
Received 18 March 2014
Received in revised form
10 January 2015
Accepted 19 January 2015

Keywords:
Finite strains
Shell elements
Pian–Sumihara stress modes
Finite strain plasticity
Least-square assumed strain

ABSTRACT

This work presents a finite strain quadrilateral element with least-squares assumed in-plane shear strains (in covariant/contravariant coordinates) and classical transverse shear assumed strains. It is an alternative to enhanced-assumed-strain (EAS) formulation and, in contrast to this, produces an element satisfying ab initio the Patch-test. No additional degrees-of-freedom are present, unlike EAS. Least-squares fit allows the derivation of invariant finite strain elements which are both in-plane and out-of-plane shear-locking free and amenable to standardization in commercial codes. With that goal, we use automatically generated code produced by AceGen and Mathematica to obtain novel finite element formulations. The corresponding exact linearization of the internal forces was, until recently, a insurmountable task. We use the tangent modulus in the least-squares fit to ensure that stress modes are obtained from a five-parameter strain fitting. This reproduces exactly the *in-plane* bending modes. The discrete equations are obtained by establishing a four-field variational principle (a direct extension of the Hu–Washizu variational principle). The main achieved goal is coarse-mesh accuracy for distorted meshes, which is adequate for being used in crack propagation problems. In addition, as an alternative to spherical interpolation, a consistent director normalization is performed. Metric components are fully deduced and exact linearization of the shell element is performed. Full linear and nonlinear assessment of the element is performed, showing similar performance to more costly approaches, often on-par with the best available shell elements.

1. Introduction

Finite strain plasticity and fracture simulations with finite elements (cf. [8,10]) are peculiarly demanding with respect to numerical efficiency, Newton iteration robustness and mesh distortion insensitivity. This is relevant in the edge-based algorithms recently proposed [12] when applied to quadrilaterals. Many of the intricate element formulations, such as enhanced-assumed-strain, hybrid stress, discrete Kirchhoff (DK, cf. [14]), are suitable for smooth problems where the mesh distortion sensitivity is not a crucial factor and governing equations do not contain discontinuities. In addition, costs associated with convergence difficulties and static condensation (specifically with EAS) can also be high. We take a different approach here: starting with a mixed 4-field functional (displacement field, director field, components of the local Cauchy–Green tensor and the corresponding stress-like Lagrange multipliers), we discretize the resulting Euler–Lagrange equations making use of suitable shape functions. A complete testing program is then performed. The set of obstacle problems for shells are the classical plate and shell benchmarks and extensions to finite strains. Testing elements in finite strains is also important since some instabilities have been found in the past (see [22] for a report with the Morley-based shell). Element technology for quadrilaterals is too vast to be accounted in a single article and many elements proposed in the last three decades vary only slightly in performance for the same number of degrees-of-freedom. Some important works must be mentioned. A milestone in the removal of transverse shear locking was achieved with the assumed natural strain (ANS) technique in 1984 and 1986 [24,36]. A decade earlier,

☆Researcher ID: **A-8849-2013**, http://www.researcherid.com/rid/A-8849-2013 Web-of-Science search: areias, p*, Link to list of Journal papers: http://home.uevora.pt/~pmaa/references.pdf.

* Corresponding author at: Department of Physics, University of Évora, Colégio Luís António Verney, Rua Romão Ramalho, 59, 7002-554 Évora, Portugal. Tel.: +351 96 3496307; fax: +351 266745394.
E-mail addresses: pareias@civil.ist.utl.pt, pmaa@uevora.pt (P. Areias).

http://dx.doi.org/10.1016/j.finel.2015.01.004
0168-874X/

in-plane bending locking was solved in 1973 by the Wilson Q6 element [51], with several ulterior corrections. For undistorted meshes, convergence rate of the results is established regardless of the incomplete higher order terms in the polynomials (see the book by Belytschko and co-workers [17]) and these higher order terms only contribute to stability and coarse-mesh accuracy. Of course, mesh distortion adversely affects the convergence rate (Lee and Bathe [31] proved the reduction of order of convergence) and it has been a problem with only a few published solution proposals, see also [7]. If the element geometry is a square or a rectangle, the present approach for in-plane bending is equivalent to the Q6 formulation. For out-of-plane shear, we adopt a consistent version of ANS. Selective integration for transverse strains has some advantages but two nearly zero-energy modes (often called spurious modes) appear in low-order symmetric quadrilateral plate elements in that case – these are known as *w*-hourglass and in-plane twist. We therefore describe the technique in the following sections. After this, both linear (four plates and four shells) and nonlinear tests(three geometrically nonlinear and two finite strain plasticity) are performed with a high degree of accuracy and mesh distortion insensitivity. Finally, conclusions are drawn in Section 7.

2. Governing equations

2.1. Static equilibrium for an arbitrary reference configuration

Cauchy equations of equilibrium for an *arbitrary reference configuration* are obtained from the corresponding *spatial* equilibrium (derivations for the latter are shown in Ogden [35]). Using standard notation (cf. [35,48]) we write the spatial equilibrium equations as

$$\frac{\partial \sigma_{ij}}{\partial x_{p_j}} + b_i = 0 \tag{1}$$

with the Cauchy tensor components σ_{ij} $(i,j=1,2,3)$. In (1) i is the direction index and j is the facet index. The components of the body force vector are b_i. In (1), coordinates x_{p_j} are the spatial, or deformed, coordinates of a given point (identified by p) under consideration. It is assumed that (1) is satisfied for a time parameter $t \in [0,T]$ with T being the total time of observation and for a point with position $\boldsymbol{x}_p \in \Omega_t$ belonging to the deformed position domain at the time of analysis. In tensor notation, Eq. (1) can be presented as

$$\nabla \cdot \boldsymbol{\sigma}^T + \boldsymbol{b} = \boldsymbol{0} \tag{2}$$

with $\nabla = \partial/\partial \boldsymbol{x}_p$ is the gradient *operator*. Making use of the deformation gradient $\boldsymbol{F}$ and the Jacobian $J = \det \boldsymbol{F}$, a direct manipulation of (1) with the use of the second Piola–Kirchhoff stress, $\boldsymbol{S} = J\boldsymbol{F}^{-1}\boldsymbol{\sigma}\boldsymbol{F}^{-T}$ leads to

$$\nabla_0 \cdot (\boldsymbol{FS})^T + J\boldsymbol{b} = \boldsymbol{0} \tag{3}$$

where ∇_0 is the gradient operator with respect to the material coordinates $\boldsymbol{x}_p$, $(\nabla_0 = \partial/\partial \boldsymbol{x}_{p0})$. A generalization results in

$$\nabla_b \cdot (\boldsymbol{F}_b \boldsymbol{S}_b)^T + J_b \boldsymbol{b} = \boldsymbol{0} \tag{4}$$

where

$$\nabla_b = \frac{\partial}{\partial \boldsymbol{x}_{pb}} \tag{5}$$

$$\boldsymbol{F}_b = \nabla_b \cdot \boldsymbol{x} \tag{6}$$

$$J_b = \det \boldsymbol{F}_b \tag{7}$$

$$\boldsymbol{S}_b = J_b \boldsymbol{F}_b^{-1} \boldsymbol{\sigma} \boldsymbol{F}_b^{-T} \tag{8}$$

Considering a time instance t_a we can re-write (4) as

$$\nabla_b \cdot (\boldsymbol{F}_{ab} \boldsymbol{S}_{ab})^T + J_{ab} \boldsymbol{b} = \boldsymbol{0} \tag{9}$$

with $\boldsymbol{F}_{ab} = \nabla_b \cdot \boldsymbol{x}_{pa}$, $\boldsymbol{S}_{ab}^T = \boldsymbol{S}_{ab}$ and $t_a \geq t_b$.

2.2. Kinematics and stress integration for displacement-based elements

Adopting (9) as the equilibrium equation with time parameters t_a and t_b, stress integration can be used in a form that avoids the polar decomposition or (explicit) objective rates. The resulting derivation can be used to achieve an efficient and robust time-integration scheme for finite plastic strains. Consider three configurations Ω_a, Ω_b and Ω_c (respectively at times $t_a \geq t_b \geq t_c$). The relative deformation gradient between two configurations Ω_a

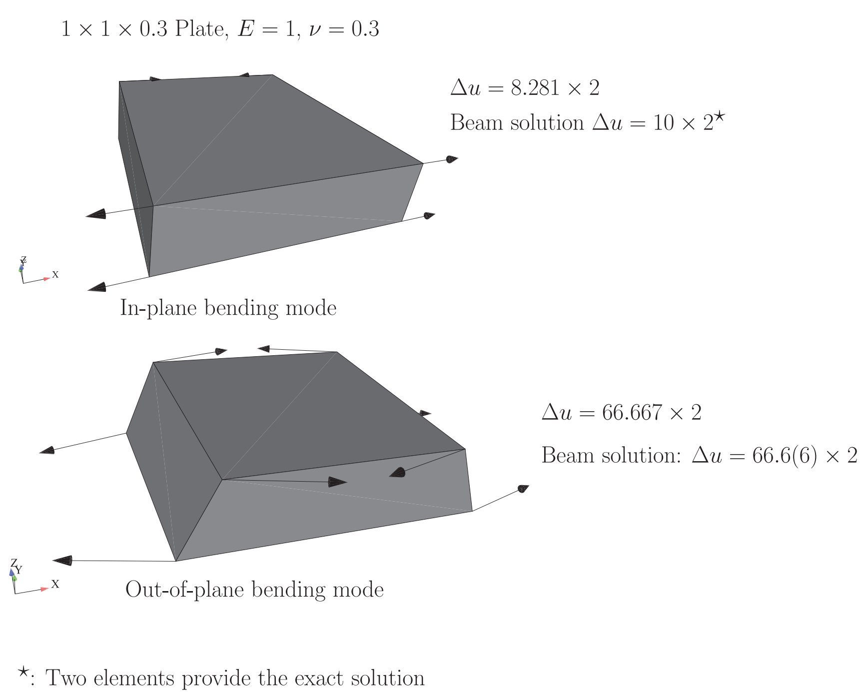

Fig. 1. In-plane and out-of-plane bending results for one shell element. Poisson effect is obtained from the use of matrix $\mathcal{L}$.